



Natural Resources Conservation Service
National Soil Survey Center
Federal Building, Room 152
100 Centennial Mall North
Lincoln, NE 68508-3866

Phone: (402) 437-5499
FAX: (402) 437-5336

Subject: Soils – Geophysical Investigations

Date: 12 August 2013

To: Joyce Swartzendruber
State Conservationist
USDA-Natural Resources Conservation Service
Federal Building, Room 443
10 East Babcock Street
Bozeman, MT 59715-4704

Purpose:

A planned NRCS project in south-central Montana will move corrals further away from a tributary of the Stillwater River and provide a vegetated buffer strip, which will prevent the runoff of nutrients and organic matter from entering the stream. The area included in this project is located within the boundaries of a National Register Site: the Crow Agency II. As part of NRCS's reasonable and good faith efforts to determine whether any archaeological features are located within the proposed relocation area, electromagnetic induction and ground penetrating radar surveys were completed across the area that will be impacted by this project.

The development, control, and reclamation of saline seeps are major concerns of management in the Northern Great Plains. A workshop was held in the Great Falls, Montana, on the use of electromagnetic induction (EMI) to identify saline seeps and recharge areas in regions of dryland farming. The use of EMI meters and measured apparent conductivity (EC_a) data to identify recharge and discharge areas associated with saline-seeps, and methods for processing, displaying and interpreting EC_a data were discussed. Field exercises allowed participants to operate EMI meters and conduct detailed and reconnaissance surveys using both mobile and pedestrian EMI.

Participants:

Craig Biggart, Soil Conservationist, USDA-NRCS, Great Falls, MT
Max Blodgett, Soil Conservationist, USDA-NRCS, Great Falls, MT
Kelli Coleman, Soil Conservation Technician, USDA-NRCS, Conrad, MT
Matt Crampton, District Conservationist, USDA-NRCS, Great Falls
Jim Doolittle, Research Soil Scientist, USDA-NRCS-NSSC, Newtown Square, PA
Stacy Enoboe, District Conservationist, USDA-NRCS, Conrad, MT
Paula Gunderson, District Conservationist, USDA-NRCS, Choteau, MT
Pat Hensleigh, State Agronomist, USDA-NRCS, Bozeman, MT
Roy Knudsen, Soil Conservation Technician, USDA-NRCS, Great Falls, MT
Cliff Merryman, District Conservationist, USDA-NRCS, Chinook, MT
Bob Nansel, District Conservationist, USDA-NRCS, Fort Benton, MT
Ted Nelson, District Conservationist, USDA-NRCS, Columbus, MT
Cari Ostberg, Area Resource Conservationist, USDA-NRCS, Great Falls MT
Dori Passmann, State Archaeologist, USDA-NRCS, Bozeman, MT
Jack Robertson, Soil Scientist, USDA-NRCS, Havre MT
Anne Stephens, Soil Conservationist, USDA-NRCS, Browning, MT
Holly Taylor, Soil Conservation Technician, USDA-NRCS, Cutbank, MT

Helping People Help the Land

An Equal Opportunity Provider and Employer



Joyce Trevithick, Area Agronomist, USDA-NRCS, Great Falls MT
Bonnie Wallace , Soil Conservation Technician, USDA-NRCS, Choteau, MT
Eric Watson Soil Conservationist, USDA-NRCS, Shelby, MT
Denise Wiedenheft, Soil Conservationist, USDA-NRCS, Bozeman, MT
Susie Wisenhart, Soil Engineering Technician, USDA-NRCS, Choteau, MT
Cory Wolfe, Civil Engineer, USDA-NRCS, Bozeman, MT

Activities:

All activities were completed between 22 and 25 July 2013.

Summary:

1. Geophysical surveys at the Crow Agency II National Register Site provided a more comprehensive coverage of the subsurface than possible with traditional archaeological field methods, detected subsurface features related previous structures and land use management by the landowner's family, and identified "areas of interest" if future archaeological excavations are required.
2. At the corral relocation site, geophysical surveys revealed no indication of pre-ranch artifacts. The integration of simultaneously recorded apparent conductivity and apparent magnetic susceptibility data proved valuable in the discrimination of pedological and anthropogenic features.
3. At a site located in Teton County, apparent conductivity maps identified the locations of not only established, but emergent saline seeps and the connectivity among them. Areas with low EC_a were associated with recharge areas. On the other hand, areas with high EC_a were associated with discharge and salt accumulation.
4. Apparent conductivity maps provide a rational approach for planning the management of saline seeps. Time-lapse EC_a surveys can be used to evaluate the extent of saline seeps and document the speed and extent of reclamation processes.
5. An Excel worksheet containing all geo-referenced EMI data that were collected at the Stillwater and Teton County sites have been forwarded to Patrick Hensleigh (State Agronomist).

It was the pleasure of Jim Doolittle and the National Soil Survey Center to work with members of your fine staff and be of assistance to you.

JONATHAN W. HEMPEL
Director
National Soil Survey Center

cc:

Sarah Bridges, Archaeologist, USDA-NRCS, Washington, DC

James Doolittle, Research Soil Scientist, Soil Survey Research & Laboratory, NSSC, MS 41, USDA-NRCS, Newtown Square, PA

William Drummond, State Soil Scientist, USDA-NRCS, Federal Building, Room 443, 10 East Babcock Street, Bozeman, MT 59715-4704

Charles Gordon, Soil Survey Regional Director, USDA-NRCS, Federal Building, Room 443, 10 East Babcock Street, Bozeman, MT 59715-4704

Patrick Hensleigh, State Agronomist, USDA-NRCS, Federal Building, Room 443, 10 East Babcock Street, Bozeman, MT 59715-4704

J. Cameron Loerch, Acting National Leader, Soil Survey Research & Laboratory, NSSC, MS 41, NRCS, Lincoln, NE

Ted Nelson, District Conservationist, USDA-NRCS, 334 N 9th Street, Columbus, MT 59019

Dori Passmann, State Archaeologist, USDA-NRCS, Federal Building, Room 443, 10 East Babcock Street, Bozeman, MT 59715-4704

David Smith, Director, Soil Science Division, USDA-NRCS, Washington, DC

Wes Tuttle, Soil Scientist (Geophysical), USDA-NRCS-NSSC, Wilkesboro, NC

Moustafa Elrashidi, Research Soil Scientist/Liaison MO4, Soil Survey Research & Laboratory, NSSC, MS 41, USDA-NRCS, Lincoln, NE

Technical Report on geophysical investigation conducted near the Crow Agency II National Register Site on 22 and 23 July 2013.

Jim Doolittle

Background:

A planned NRCS project at the Ostrum's family ranch in south-central Montana will move an animal feeding operation (AFO) further away from a tributary of the Stillwater River and provide a wider vegetated buffer strip, which will help to prevent the runoff of nutrients and organic matter from entering the stream. The area included in this project is located within the boundaries of a National Register Site: the Crow Agency II. While the full extent of this archaeological site is unknown, due diligence is required by NRCS to identify archaeological features located within the area that will be impacted by the coral relocation project.

In addition, the Ostrum family has a project that will involve the conversion of flood irrigation to sprinkler irrigation systems. This proposed project will increase the irrigation efficiency by at least 30%. The present method of irrigation is a combination of gated pipe and contour ditches on a field that isn't level. The proposed sprinklers will help to eliminate runoff, reduce deep percolation, and improve plant health and productivity. The project will involve a structure to filter the water, buried delivery pipes, a pumping plant, two center pivot sprinklers, and the implementation of irrigation water management and forage harvest management plans.

NRCS is committed to the protection and enhancement of our nation's cultural resources and historic properties. As part of NRCS's reasonable and good faith efforts to determine whether any archaeological features are located within these sites, Dori Passmann, the NRCS State Archaeologist, requested geophysical assistance from the National Soil Survey Center's Soil Survey Research and Laboratory Staff. With the assistance of the Montana State Office, the Columbus NRCS Field Office, and the Montana Resource Planning and Implementation Team, electromagnetic induction (EMI) and ground penetrating radar (GPR) surveys were completed across the area that will be impacted by the proposed coral relocation project, and an EMI survey was completed along the proposed route of the irrigation delivery pipes.

Spatial variations in apparent conductivity (EC_a) and apparent magnetic susceptibility (MSa) were measured with an EM38-MK2 meter and used to identify areas with potential "cultural loading" (Dalan and Bevan, 2002). As shown in this report, the use of both EC_a and MSa data can significantly improve interpretation. Differences in MSa and EC_a have been used as indicators of human occupation and soil disturbance (Simpson et al., 2009).

The measurement of apparent magnetic susceptibility with EMI meters is not common. Though principally associated with soil mineralogy (Magiera et al., 2006) and the presence of ferromagnetic minerals (Mullins, 1977), magnetic susceptibility has also been associated with soil particle size distributions, organic matter and moisture contents (Maier et al., 2006; Mullins, 1977). Magnetic susceptibility has been observed to vary with slope positions (de Jong et al., 2000), soil drainage (Maier et al., 2006), and vegetation (Dearing et al., 1996).

In addition, local variations in apparent magnetic susceptibility have been associated with anthropogenic disturbances (Clark, 1990; Dalan and Banerjee, 1996). Variations in MSa has been used to identify and map hearths, waste heaps, charcoal, bricks, structures, trenches and areas with dispersed cultural debris (De Smedt et al, 2013a and 2013b; Saey et al., 2013; Viberg et al., 2013; Simpson et al., 2009). Studies conducted by Dalan (2006) in North Dakota and Minnesota associated magnetic responses to nodules of

burnt clay at prehistoric archaeological sites. Magnetic studies conducted by Kvamme and Ahler (2007) on an earthen lodge village in North Dakota, revealed pits, hearths, midden deposits, trails, refilled fortification ditches, bastions, houses, and burrow pits. Dalan (2007) noted that structures (e.g., walls) are often identified by linear magnetic differences (usually highs). As a caveat, it must be emphasized that excavations of some magnetic anomalies have provided no indication of the sources of the anomalies as measured responses only indicated differences in M_{Sa}, which may or may not be associated with archaeological features.

Equipment:

An EM38MK2 meter (Geonics Limited; Mississauga, Ontario) was used in this investigation¹. This meter requires no ground contact and only one person to operate. The EM38-MK2 meter operates at a frequency of 14,500 Hz and weighs about 5.4 kg (11.9 lbs). The meter has one transmitter coil and two receiver coils, which are separated from the transmitter coil at distances of 1.0 and 0.5 m. By rotating the EM38-MK2 meter, it can be positioned in either the deeper-sensing vertical (VDO) or shallower-sensing horizontal (HDO) dipole orientation.

In either dipole orientation, the EM38-MK2-2 meter provides simultaneous measurements of both EC_a and M_{Sa}. The quadrature phase signal response is representative of soil EC_a and is expressed in milliSiemens/meter (mS/m). Apparent conductivity is principally influenced by variations in soil soluble salts, clay, and/or water contents. It is also influenced by a combination of physio-chemical properties that include: organic matter, clay mineralogy, cation exchange capacity, bulk density, and temperature. The depth of investigation (DOI) is universally taken at the depth of 70 % cumulative response. This theoretical assumption results in DOI of about 1.5 and 0.75 m when the meter is operated in the VDO, and about 0.75 and 0.40 m when operated in the HDO.

The in-phase response is representative of soil M_{Sa}. Susceptibility is the ratio of the secondary to primary magnetic fields and is expressed in parts per thousand (ppt). The apparent magnetic susceptibility of earthen materials depends on the magnetic concentration, composition (type of minerals) and grain size (Dalan, 2007). The maximum sensitivity of the in-phase component (M_{Sa}) is reached approximately 0.2 m below the instrument, but it can detect features down to depths of approximately 0.5 m (Geonics Limited, 2009, Dalan, 2006; Clark, 1996). Operating procedures for the EM38-MK2 meter are described by Geonics Limited (2009).

A Trimble AgGPS 114 L-band DGPS (differential GPS) antenna (Trimble, Sunnyvale, CA) was used to georeferenced the EMI data.¹ The RTM38MK2 program (Geomar Software, Inc., Mississauga, Ontario) was used to display and record both GPS and EMI data on an Allegro CX field computer (Juniper Systems, North Logan, Utah).¹

To help summarize the results of the EMI surveys, the SURFER for Windows (version 10.0) software program (Golden Software, Inc., Golden, CO) was used to construct the simulations shown in this report.¹ Grids were created using kriging methods with an octant search.

A TerraSIRch Subsurface Interface Radar (SIR) System-3000 (here after referred to as the SIR-3000), manufactured by Geophysical Survey Systems, Inc. (GSSI; Salem, NH), was used in the investigation at the AFO.¹ The SIR-3000 consists of a digital control unit (DC-3000) with keypad, SVGA video screen, and connector panel. A 10.8-volt lithium-ion rechargeable battery powers the system. The SIR-3000 weighs about 4.1 kg (9 lbs) and is backpack portable. With an antenna, the SIR-3000 requires two people to operate. Jol (2009) and Daniels (2004) discuss the use and operation of GPR. A relatively high frequency, 400 MHz antenna was used in the investigation.

¹ Manufacturer's names are provided for specific information; use does not constitute endorsement.

The RADAN for Windows (version 7.0) software program (developed by GSSI) was used to process the radar records.² Processing procedures used included: header editing, setting the initial pulse to time zero, color table and transformation selection, signal stacking, horizontal high pass filtration, and migration (refer to Jol (2009) and Daniels (2004) for discussions of these techniques). These processing techniques were used to improve pattern recognition.

Animal Feeding Operation (AFO) relocation site:

Survey Area:

The AFO relocation site is located in Stillwater County, Montana, about 350 m southeast of the intersection of State Highways 78 and 419. The site is about 5.2 km south of Absarokee and 5.0 km northeast of Fishtail.



Figure 1. This soil map of the animal feeding operation relocation site shows the area surveyed with the EM38-MK2 meter.

Figure 1 is a soil map of the survey area. This soil map is from the Web Soil Survey.³ Soil delineations included in the relocation area are Lohler clay loam, 2 to 4 % slopes (36); Lolo and Nesda soils, flooded in (38); and Turner clay loam, 2 to 4 % slopes (58). The taxonomic classifications of these soils are listed in Table 1. These very deep soils form in alluvium on stream terraces and flood plains. The well drained to moderately well drained Lohler soils formed in stratified clayey alluvium. The 10- to 40-inch control section of Lohler soils typically averages 45 and 60 percent clay. The well drained Lolo and Nesda soils

² Manufacturer's names are provided for specific information; use does not constitute endorsement.

³ Soil Survey Staff, Natural Resources Conservation Service, United States Department of Agriculture. Web Soil Survey. Available online at <http://websoilsurvey.nrcs.usda.gov/>. Accessed [07/30/2013].

formed in gravelly alluvium derived from mixed rock sources. The well drained Turner soils have strata of sands and gravel at a depth of 20 to 40 inches.

Table 1. Taxonomic classification of the named soils at the AFO relocation site.

Soil Series	Taxonomic Classification
Lohler	Fine, smectitic, calcareous, frigid Vertic Ustifluvents
Lolo	Loamy-skeletal, mixed, superactive, frigid Pachic Haplustolls
Nesda	Sandy-skeletal, mixed, frigid Fluventic Haplustolls
Turner	Fine-loamy over sandy or sandy-skeletal, mixed, superactive, frigid Typic Argiustolls

Survey procedures:

The EMI surveys were completed by randomly walking across all open and accessible areas of the relocation site with the EM38-MK2 meter held in the VDO, about 5 cm above the ground surface, and with its long axis parallel with the direction of traverse. Where possible, metal fences, gates, and post were not approached closer than 2 meters in order to avoid electromagnetic interference. The reported EC_a data were not corrected to a standard temperature.

Results:

Table 2 provides basic statistics for the EMI data collected with the EM38-MK2 meter at the AFO relocation site. In general, apparent conductivity increased with increasing depth of investigation. For the deeper-sensing measurements collected with the 100-cm intercoil spacing (100 EC_a), EC_a averaged 34.5 mS/m and range from about -17 to 171 mS/m. However, one-half of the EC_a measurements were between about 21 and 45 mS/m. For the shallower-sensing measurements collected with the 50-cm intercoil spacing (50 EC_a), EC_a averaged 24.5 mS/m and ranged from -75 to 313 mS/m. However, one-half of the EC_a measurements were between about 12 and 35 mS/m. For both sets of EC_a measurements, the extreme range in EC_a is associated with the presence of manure, metal fencing, and assorted cultural features and debris.

Table 2. Basic statistics for the EMI data collected with the EM38-MK2 meter at the AFO relocation site. Apparent conductivity and in-phase response are expressed in mS/m and ppt, respectively.

	100 EC _a	50 EC _a	100 IP	50 IP
Number	6654	6654	6654	6654
Minimum	-16.6	-75.0	-284.1	-26.5
25%-tile	20.9	11.7	11.9	17.7
75%-tile	44.9	35.2	25.7	56.8
Maximum	170.7	313.0	783.3	987.5
Mean	34.5	24.5	20.6	37.8
St. Dev.	17.3	18.8	21.9	30.3

The average in-phase (IP) response (MSa) decreased and became less variable with increasing intercoil spacing and supposedly increasing depths of investigation. The apparent magnetic susceptibility averaged 37.8 and 20.6 ppt for measurements recorded with the 50 and 100-cm intercoil spacings, respectively. The IP response ranged from about -26 to 988 ppt and from -284 to 783 ppt for measurements recorded with the 50- and 100-cm intercoil spacings, respectively. The extreme range in IP measurements is associated with the presence of metallic artifacts. However, one-half of the IP measurements were between about 18 and 57 ppt for the 50-cm intercoil spacing and between about 12 and 26 ppt for the 100-cm intercoil spacing.

Figure 2, contains plots of EC_a data collected at the AFO relocation site. The same color scale and scheme are used in each plot. The upper and lower plots represent spatial EC_a data recorded in the shallower-sensing 50-cm and the deeper-sensing 100-cm intercoil spacing, respectively. In each plot, white lines have been used to identify the approximate location of metal fences that partitioned the study area into different corrals (labeled C, D, and E) and fields (labeled A and B). In both plots, anomalously high EC_a values are associated with piles of animal waste (the locations of two piles have been identified by ellipses of segmented lines in corral C and D). In corral E, two piles were observed during the survey, but have not been identified in Figure 2.

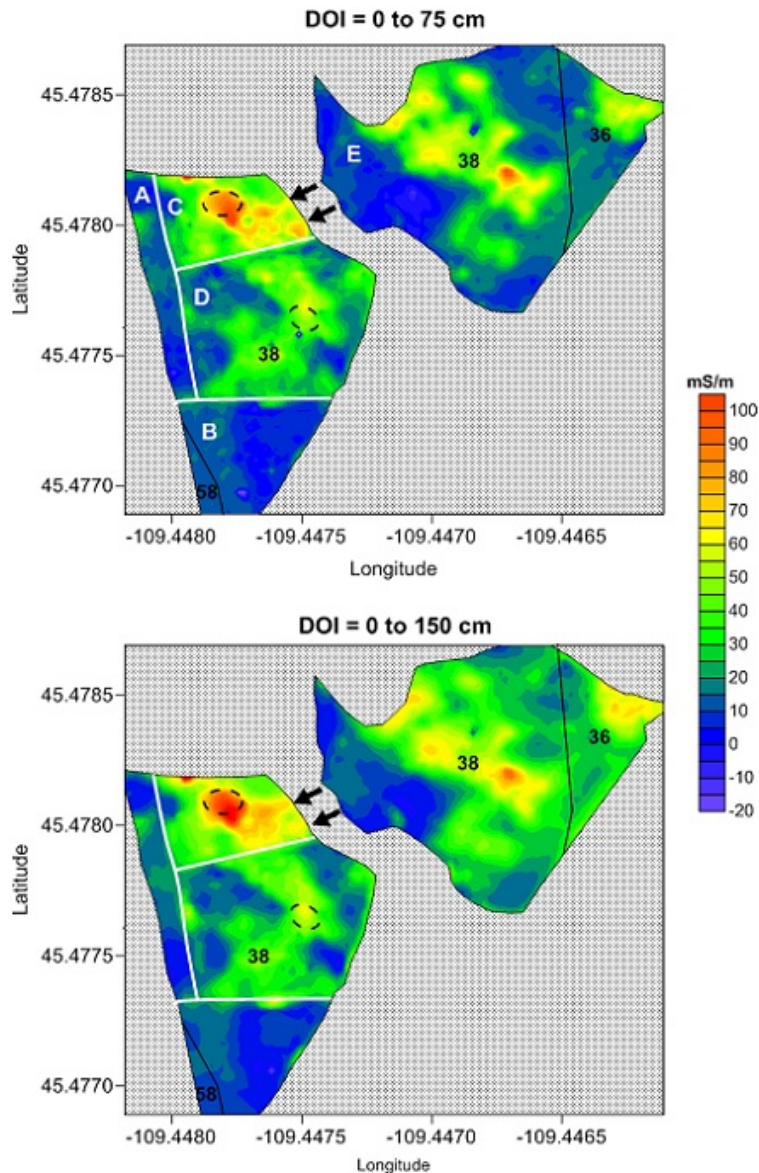


Figure 2. These plots from the AFO relocation site depict the EC_a data collected with the shallower-sensing 50- (top plot) and the deeper-sensing 100-cm (bottom plot) intercoil spacing of the EM38-MK2 meter operated in the VDO.

In the plots shown in Figure 2, EC_a is noticeably higher in the three corrals (C, D, and E) that are used as loafing areas for horses and the storage of excess wastes (manure piles). The higher EC_a in the corrals contrasts with the lower EC_a in the adjoining fields (A & B). The higher EC_a is attributed to the greater

concentration of nutrients from the animal waste. Fields that are located to the south (B) and west (A) of the corrals have noticeably lower concentrations of waste products and lower EC_a . In the plot shown in Figure 2, arrows have been used to indicate where spatial patterns suggest plumes of higher EC_a (and associated contaminants) are entering Butcher Creek. In the plots shown in Figure 2, many spatial EC_a patterns have a distinct linearity that suggests artificial rather than natural features, which are seldom linear and generally more irregular in geometry.

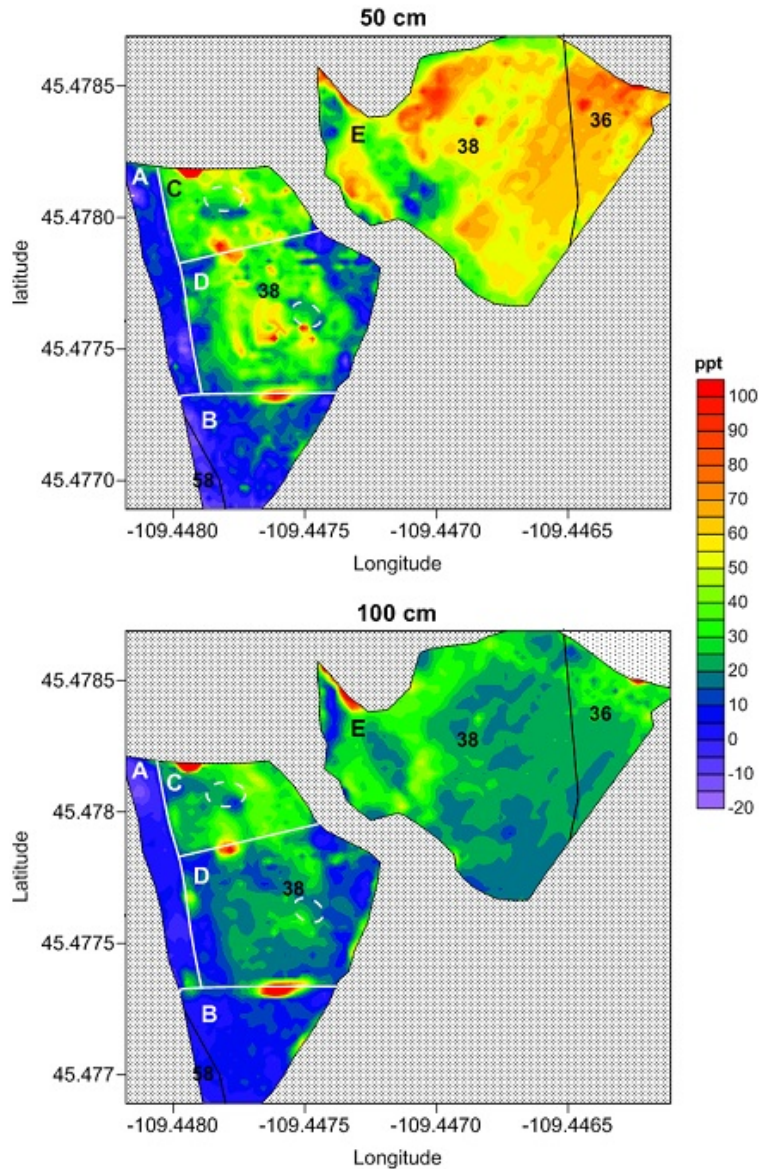


Figure 3. These plots from the AFO relocation site depict the MSa data collected with 50- (upper plot) and 100-cm (lower plot) intercoil spacing of the EM38-MK2 meter operated in the VDO.

Figure 3, contains plots of IP data collected at the AFO relocation site. The same color scale and scheme are used in both plots. The upper and lower plots represent spatial IP data recorded with the 50-cm and the 100-cm intercoil spacing, respectively. In each plot, white lines have been used to identify the approximate location of metal fences that partitioned the study area into different corrals (labeled C, D, and E) and fields (labeled A and B). Several anomalously high IP values (outliers) can be observed along

segments of these fence lines and the northern and northeastern borders of corral E. These represent areas of electromagnetic interference from fence lines that were approached too closely by the EMI meter.

In Figure 3, spatial variations in the IP response or the MSA measured with an EM38-MK2 meter can be used to identify areas of “cultural loading” (Dalan and Bevan, 2002). Large areas with what is believed to be “culturally disturbed or modified” soils, which display more anomalously high and low MSA, are evident in the plots shown in Figure 3 and appear to extend over a larger area than was outlined from the EC_a data presented in Figure 2. In Figure 3, linear spatial patterns are more prominent in the 50-cm intercoil spacing measurements. These patterns suggest major differences in land use and management, and the possible presence of walls, fence and utility lines. It is evident in these plots and from the recorded data that levels of magnetic susceptibility decrease and become less variable with increasing soil depth. This trend is believed to represent *cultural loading* of surface layers (Dalan and Bevan, 2002; Bevan, 1994).

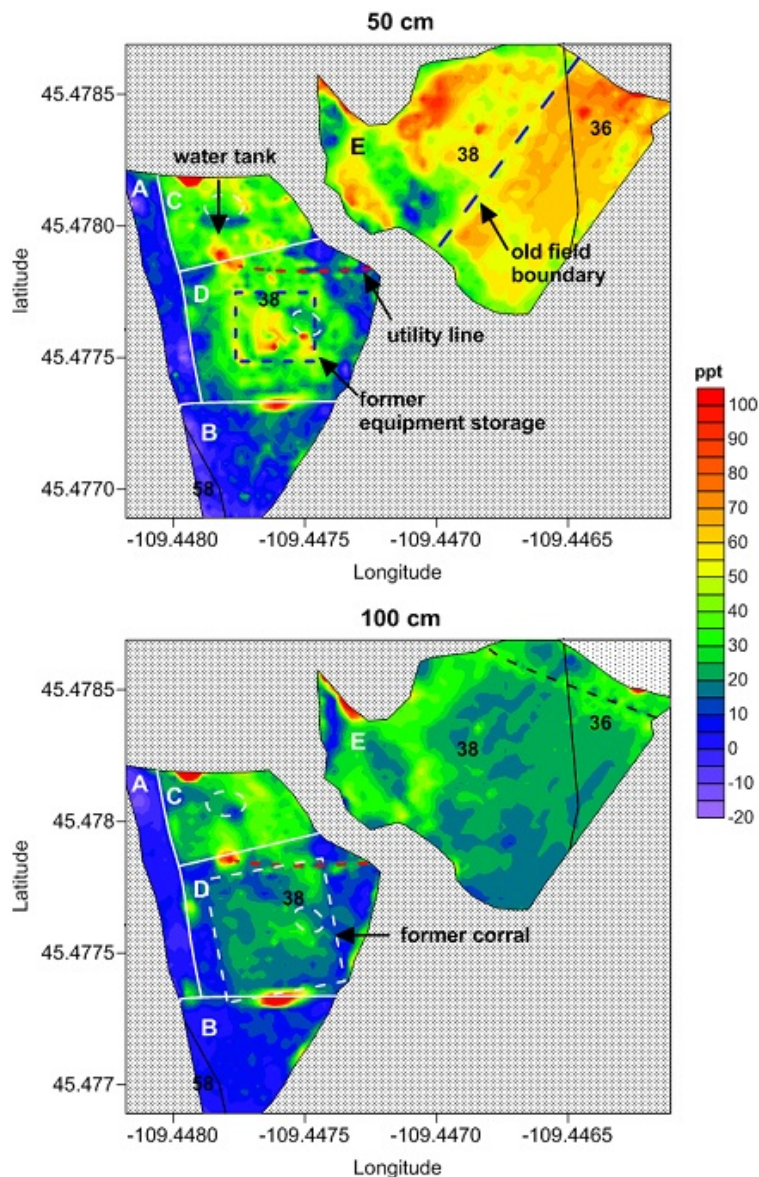


Figure 4. Present and former cultural features known by the landowner are identified in these plots of MSA data from the AFO relocation site.

During an exist interview, the landowner identified many of the spatial features labeled in the IP plots shown in Figure 4. In each plot, the anomalous values are believed to represent cultural features and debris remnant from activities of the present landowner and his predecessors. While no clear outline of former structures or features are identifiable on these plots, linear and rectangular spatial patterns suggest artificial rather than natural features.

Pedological constraints (clay contents, CEC, soil moisture, nutrients from animal waste) of the site should have excluded the use of GPR. However, exploratory surveys were carried out with GPR. Multiple passes were made with the GPR in the area to the immediate north and south of the manure pile in corral D (see Figures 2 to 4). These traverses were orientated in an east to west direction. Five parallel traverses (each 56 m long and spaced 60 cm apart) were completed in the area to the immediate north of a manure pile. Five parallel traverses (each 49 m long and spaced 60 cm apart) were completed in the area to the immediate south of a manure pile in corral D.

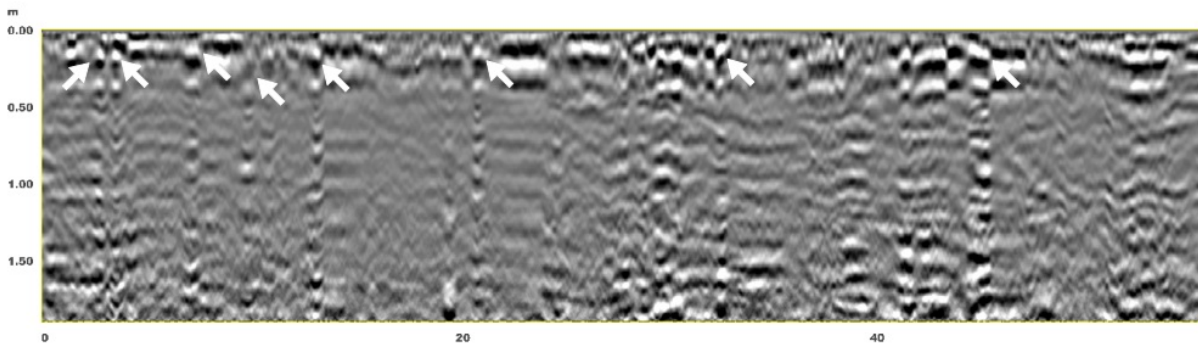


Figure 5. A representative radar record collected with a 400 MHz antenna in corral D. All scales are expressed in meters.

Figure 5 is a representative radar record of one of the traverse lines. This traverse line is 56 m long. Velocity of pulse propagation through the sediment and the resulting depth scale were determined by hyperbola fitting analysis. Hyperbola fitting procedures examine the GPR data and calibrate the velocity by adjusting a graphic hyperbola to match hyperbola reflectors on the GPR record.

The radar record shown in Figure 5 is of poor interpretative quality because of highly attenuating soil conditions (high nutrient, clay and soluble salt levels). Subsurface interfaces are not clearly expressed. Metallic point objects and jarring of the antenna as it passed over obstacles on the ground surface produced unwanted noise that reverberates downward on the radar record (identified by white arrows in Figure 5). No identifiable radar reflection pattern was recognized. Interpretations of the 2D radar records from this site were inconclusive.

In recent years, the use of advanced signal-processing software has enabled the enhancement of radar signals and significant improvements in the recognition of reflection patterns on radar records. Some of the signal processing methods that have been used to improve the interpretability of subsurface cultural features appearing on radar records are discussed by Sciotti et al. (2003) and Conyers (2004). One advanced signal processing method that is commonly used in archaeological investigations is amplitude-slice analysis (Conyers, 2004). This analysis explores differences in signal amplitudes within a 3D pseudo-image, which has been constructed from the fusion of multiple, closely-spaced, parallel radar records, in "time-slices" (or depth-slices). In each time-sliced image, the reflected radar energy is averaged horizontally between adjacent, parallel radar traverses and in specified time (or depth) windows.

Each amplitude time-slice image shows the distribution of reflected signal amplitudes within a specific depth interval (Conyers, 2004). These patterns can indicate changes in soil properties, distinguish and identify potential artifacts, and reduce interpretation uncertainties.

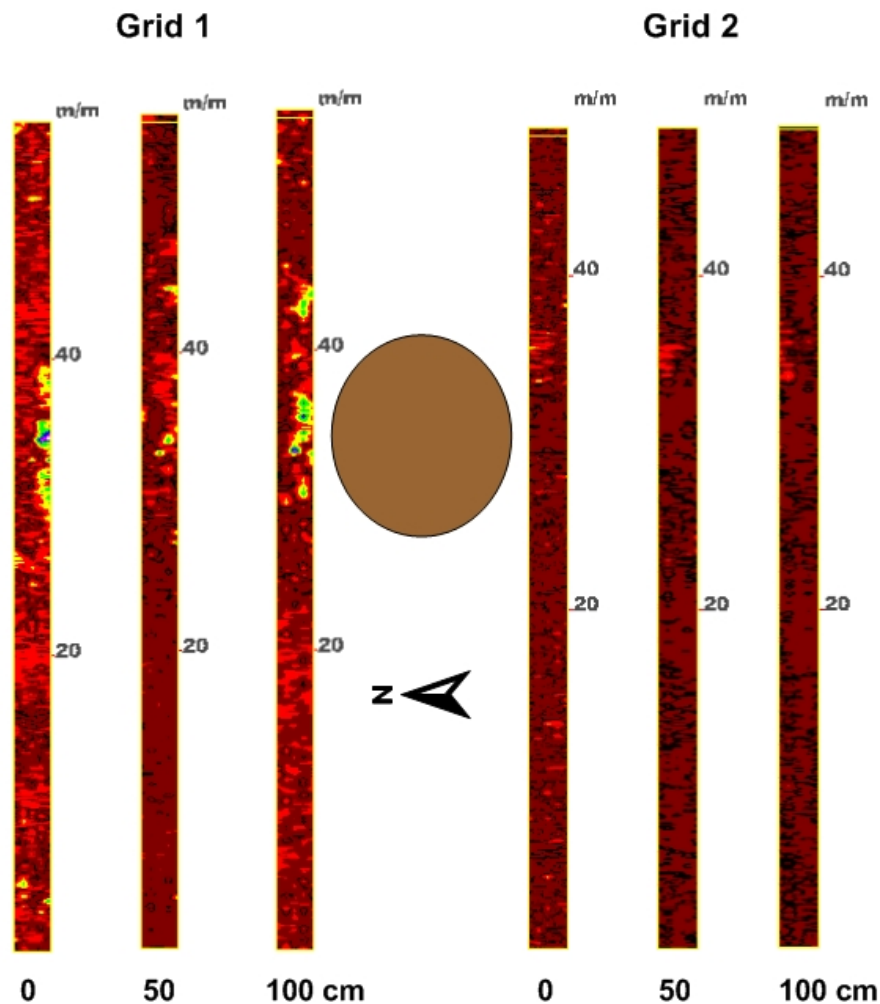


Figure 6. These depth sliced images are for two very narrow grid areas in Corral D. For each grid, three depth-sliced images have been prepared for the 0, 50, and 100-cm depth intervals.

Figure 6 contains two sets of time- or depth-sliced images based on the 3D pseudo images created from radar traverses conducted on either side of the manure pile in corral D. For each grid, GPR data were collected along a series of 5, closely spaced (60 cm) parallel traverse lines. Traverse line lengths were 56 and 49 m for Grids 1 and 2, respectively. These procedures produced a 56 by 2 m (112 m²) and a 49 by 2 m (98 m²) 3D pseudo-image for Grids 1 and 2, respectively. For each grid, three depth-sliced images are shown. Depth-sliced images are for the 0, 50 and 100-cm depth intervals. In Figure 6, the two grid areas are viewed from directly overhead with succeeding depth slice images arranged to the right. The approximate location of a manure pile is shown in Figure 6. Several clusters of high-amplitude reflections are evident in Grid 1. These high-amplitude spatial patterns are irregular, do not necessarily suggest buried cultural features, and are inconclusive. Buried structures and graves generally have a more confined linear expression. These patterns suggest an “areas of interest” that may warrant further inspection by an archaeological if exploratory excavations are required.

Sprinkler irrigation system site:

The proposed sprinkler irrigation site is located in Stillwater County, Montana, about 1.2 km southeast of the intersection of State Highways 78 and 419. The site is located about 820 m southeast of the AFO relocation site.



Figure 7. This soil map of the proposed site for a sprinkler irrigation system shows the narrow areas that were surveyed with the EM38-MK2 meter.

Figure 7 is a soil map of the survey area. This soil map is from the Web Soil Survey⁴. The survey area lies entirely within a delineation of Lohler clay loam, 2 to 4 % slopes (36). Other soils listed as minor components in this map unit (Work, Havre, and Turner) are very similar chemically with salinity up to 4.0 and a sodium adsorption ratio of zero.

Survey procedures:

Multiple, closely spaced traverses were completed along the proposed alignment of the buried pipelines for the pivots (see Figure 7) with the EM38-MK2 meter held in the VDO, about 5 cm above the ground surface, and with its long axis parallel to the direction of traverse.

Results:

Table 3 provides basic statistics for the EMI data collected with the EM38-MK2 meter at the sprinkler irrigation site. In general, EC_a increased with increasing depth of investigation. For the deeper-sensing measurements collected with the 100-cm intercoil spacing (100 EC_a), EC_a averaged 26.6 mS/m and ranged from about -340 to 148 mS/m. However, one-half of these EC_a measurements were between about 21 and 29 mS/m. For the shallower-sensing measurements collected with the 50-cm intercoil spacing (50 EC_a), EC_a averaged 16.2 mS/m and ranged from about -609 to 171 mS/m. However, one-half of these EC_a measurements were between about 12 and 19 mS/m. These vertical differences in EC_a can be attributed principally to increasing soluble salts, moisture and/or clay contents within increasing soil

⁴ Soil Survey Staff, Natural Resources Conservation Service, United States Department of Agriculture. Web Soil Survey. Available online at <http://websoilsurvey.nrcs.usda.gov/>. Accessed [07/30/2013].

depths. The extreme range in EC_a is believed to be associated with the presence of metallic features and debris scattered across the site.

Table 3. Basic statistics for the EMI data collected with the EM38-MK2 meter at the proposed sprinkler irrigation site. Apparent conductivity (EC_a) and in-phase response (IP) are expressed in mS/m and ppt, respectively.

	100 EC_a	50 EC_a	100 IP	50 IP
Number	9108	9108	9108	9108
Minimum	-339.9	-608.6	-426.3	-175.2
25%-tile	21.2	11.8	9.5	9.5
75%-tile	28.8	18.6	12.8	26.3
Maximum	147.6	170.9	126	1220
Mean	26.6	16.2	11.2	19.1
St. Dev.	15.1	15.4	9.6	21.5

The average IP response (MSa) decreased and became less variable with increasing intercoil spacing and supposedly increasing depths of investigation. The apparent magnetic susceptibility averaged 19.1 and 11.2 ppt for measurements recorded with the 50 (50 IP) and 100 (100 IP) cm intercoil spacings, respectively. The IP response ranged from about -175 to 1220 ppt and from -426 to 126 ppt for measurements recorded with the 50- and 100-cm intercoil spacings, respectively. However, for each set of measurements, the interquartile range was much more restricted. One-half of the IP measurements were between about 10 and 26 ppt for the 50-cm intercoil spacing and between about 10 and 13 ppt for the 100-cm intercoil spacing. The extreme range in IP response is believed to be associated with the presence of metallic features and debris scattered across the site.

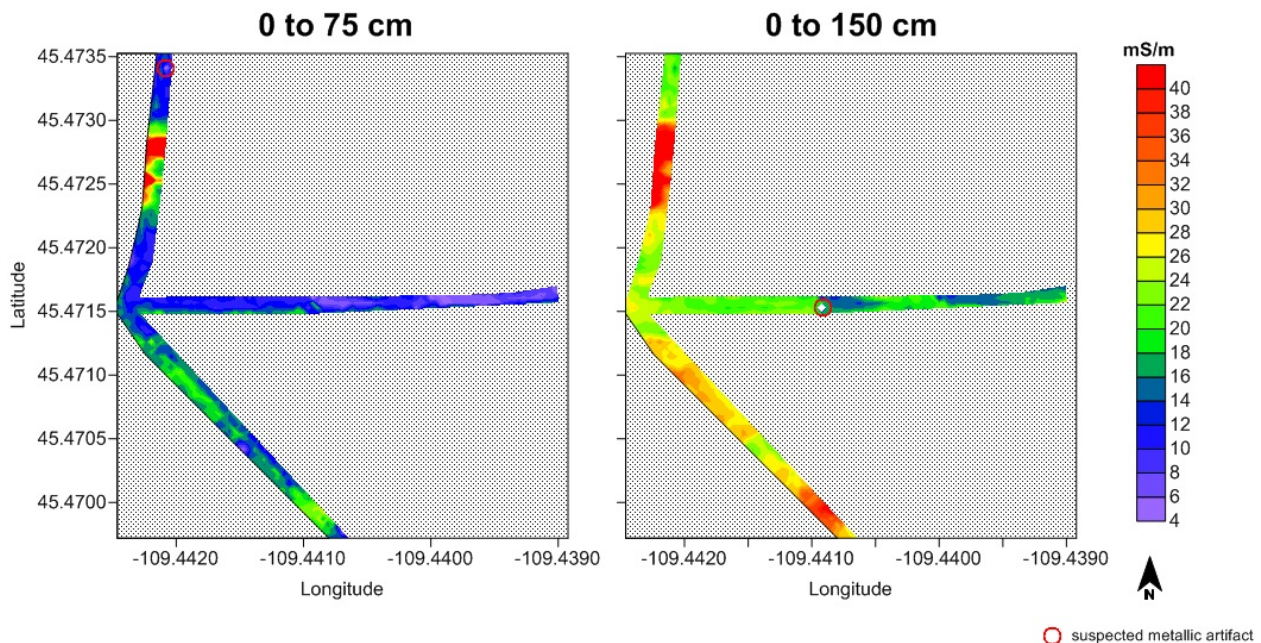


Figure 8. These plots of the proposed sprinkler irrigation site depict the apparent conductivity data collected with 50- (left-hand plot) and 100-cm (right-hand plot) intercoil spacing of the EM38-MK2 meter operated in the VDO.

Figure 8, contains plots of EC_a data collected at the proposed sprinkler irrigation site. For comparative purposes, the same color scale and scheme are used in both plots. The left-hand and right-hand plots represent the spatial EC_a data recorded in the shallower-sensing 50-cm and the deeper-sensing 100-cm

intercoil spacing, respectively. Although the survey area was restricted, several generalizations can be. Apparent conductivity increased in a downslope direction (from east to west). Though not recognized on the soil map, areas of higher EC_a (>30) may represent wet spots or patches with higher soluble salt contents. Anomalously high and low values (off the scale shown in Figure 8) are believed to represent metallic artifacts placed or discarded across the site (see red colored ellipses in Figure 8).

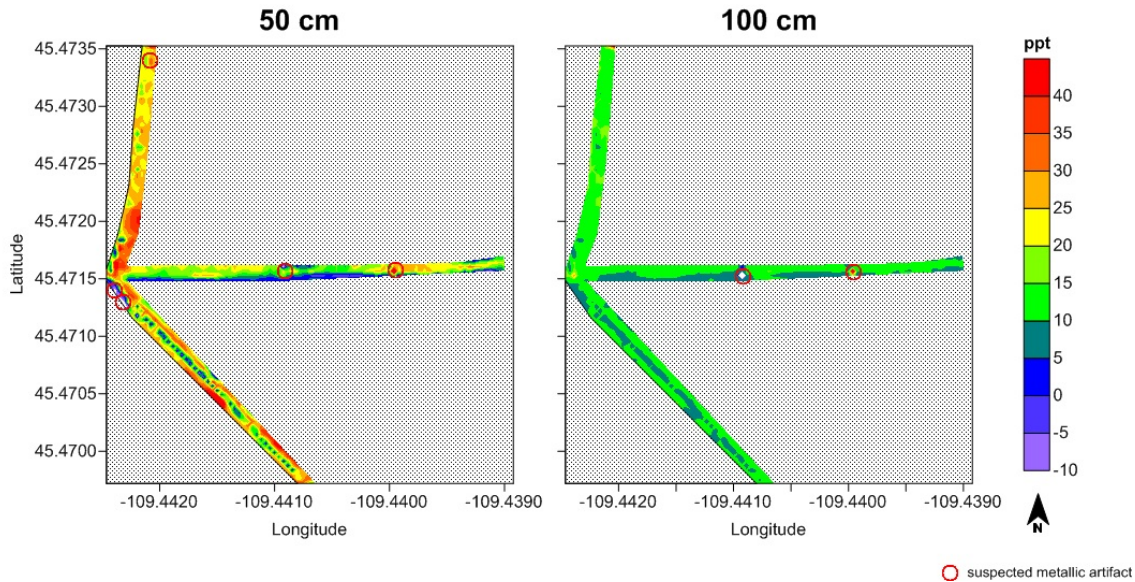


Figure 9. These plots of the proposed sprinkler irrigation site depict the apparent magnetic susceptibility for the data collected with 50- (left-hand plot) and 100-cm (right-hand plot) intercoil spacing of the EM38-MK2 meter operated in the VDO.

Figure 9, contains plots of MSa data collected at the proposed sprinkler irrigation site. For comparative purposes, the same color scale and scheme are used in both plots. The left-hand and right-hand plots represent spatial MSa (IP) data recorded in the 50-cm and the 100-cm intercoil spacing, respectively. Apparent magnetic susceptibility is higher along the lower-lying, western perimeter of the survey area. However, without further field measurements, no explanation for these spatial patterns is possible at this time.

A closer examination of the apparent magnetic susceptibility plots shown in Figure 9 reveals a linear pattern of low IP values that appears to correspond with a traverse line. As operators were switched for each traverse, it is possible that these lines represent electromagnetic interference caused by metallic objects on one of the operators.

References:

Bevan, B., 1994. Remote sensing of gardens and fields. 70-90 pp. In: Miller, N. F., and K. L. Gleason (Eds.), *The Archaeology of Gardens and Fields*, University of Pennsylvania Press, Philadelphia, PA.

Clark, A. 1990. *Seeing Beneath the Soil – Prospecting Methods in Archaeology*. Routledge, Abingdon, UK.

Clark, A., 1996. *Seeing beneath the Soil. Prospecting Methods in Archaeology*. Batsford Ltd, London.

Conyers, L.B., 2004. *Ground-Penetrating Radar for Archaeology*. Altamira Press, Walnut Creek, California (2004)

- Dalan, R.A. 2006. A geophysical approach to buried site detection using down-hole susceptibility and soil magnetic techniques. *Archaeological Prospection* 13(3):182-206.
- Dalan, R.A. 2007. A review of the role of magnetic susceptibility in archaeological studies in the USA: Recent Developments and prospects. *Archaeological Prospection* 15: 1-31.
- Dalan, R.A. and S.K. Banerjee, 1996. Soil magnetism, an approach for examining archaeological landscapes. *Geophysical Research Letters* 23(2): 185-188.
- Dalan, R.A., and B.W. Bevan, 2002. Geophysical indicators of culturally emplaced soils and sediments. *Geoarchaeology: An International Journal* 17(8): 779-810.
- Daniels, D.J., 2004. *Ground Penetrating Radar; 2nd Edition*. The Institute of Electrical Engineers, London, United Kingdom.
- Dearing, J. A., K. L. Hay, S. M. J. Baban, A. S. Huddleston, E. M. H. Wellington, and P. J. Loveland, 1996. Magnetic susceptibility of soil: an evaluation of conflicting theories using a national data set. *Geophysical Journal International* 127: 728-734.
- De Jong, E., D.J. Pennock, and P.A. Nestor, 2000. Magnetic susceptibility of soils in different slope positions in Saskatchewan, Canada. *Catena* 40: 291-305.
- De Smedt, P., M. Van Meirvenne, N.S. Davies, M. Bats, T. Saey, J. Du Reu, E. Meerschman, V. Gelorini, A. Zwertvaegher, M. Antrop, J. Bourgeois, P. De Maeyer, P.A., Finke, J. Verniers, and P. Crombé, 2013a. A multidisciplinary approach to reconstructing Late Glacial and Early Holocene landscapes. *Journal of Archaeological Science* 40: 1260-1267.
- De Smedt, P., T. Saey, A. Lehouck, B. Stichelbaut, E. Meerschman, M. Monirul Islam, E. Van De Vijver, and M. Van Meirvenne, 2013b. Exploring the potential of multi-receiver EMI survey for geoarchaeological prospection: A 90 ha dataset. *Geoderma* 199: 30-36.
- Geonics Limited. 2009. EM38-MK2-1 ground conductivity meter operating manual. Geonics Ltd., Mississauga, Ontario.
- Jol, H., 2009. *Ground Penetrating Radar: Theory and Applications*. Elsevier Science, Amsterdam, The Netherlands.
- Kvamme, K., and S. Ahler, 2007. Integrated remote sensing and excavation at Double Ditch State Historical Site, North Dakota. *American Antiquity* 72(3): 539-561.
- Magiera, T., Z. Strzyszczyk, A. Kapička, and E. Petrovský, 2006. Discrimination of lithogenic and anthropogenic influences on topsoil magnetic susceptibility in Central Europe. *Geoderma* 130: 299-311.
- Maier G., R. Scholger, and J. Schön, 2006. The influence of soil moisture on magnetic susceptibility measurements. *Journal of Applied Geophysics* 59: 162-175.
- Mullins, C. E., 1977. Magnetic susceptibility of the soil and its significance in soil science. A review. *Journal of Soil Science* 28: 223-246.

Saey, T., B. Stichelbaut, J. Bourgeois, V. Van Eetvelde, and M. Van Meirvenne, 2013. An interdisciplinary non-invasive approach to landscape archaeology of the Great War. *Archaeological Prospection* 20: 39-44.

Sciotti, M., F. Colone, D. Pastina, and T. Bucciarelli, 2003. GPR for archaeological investigations: Real performance assessment for different surface and subsurface conditions. 2266-2268 pp. IN: Proceedings 2003 IEEE International Geoscience and Remote Sensing (IGARSS 2003), 21-25 July 2003, Toulouse, France.

Simpson, D., A. Lehouck, L. Verdonck, H. Vermeersch, M. Van Meirvenne, J. Bourgeois, E. Thoen, and R. Doctor. 2009. Comparison between electromagnetic induction and fluxgate gradiometer measurements on the buried remains of a 17th century castle. *Journal of Applied Geophysics* 68 (2): 294-300.

Viberg, A. A. Berntsson, and K. Lidén, 2013. Archaeological prospection of a high altitude Neolithic site in the arctic mountain tundra region of Sweden. *Journal of Archaeological Science* 40: 2579-2588.

Technical Report on EMI and Saline Seep Workshop, held in Great Falls, Montana on 24 and 25 July 2013.

Jim Doolittle

The development, control, and reclamation of saline seeps are major concerns of management in the Northern Great Plains. On 24 and 25 July 2013, a workshop was held on the use of electromagnetic induction (EMI) to identify saline seeps and recharge areas in regions of dryland farming. Twenty agronomists, conservationists, soil scientists, and technicians from north-central Montana attended the two-day workshop in the Great Falls, Montana. The use of EMI meters and measured apparent conductivity (EC_a) data to identify recharge and discharge areas associated with saline-seeps, and methods for processing, displaying and interpreting EC_a data were discussed. Field exercises allowed participants to operate EMI meters, and conduct detailed and reconnaissance surveys using both mobile and pedestrian EMI platforms over a 160-acre field that contained saline seeps in Teton County (see Figure 1).



Figure 1. This image shows the study site in Teton County.

Background:

Saline seeps are areas of groundwater discharge in dryland farming regions. Saline seeps develop when excess water that is not absorbed by plants moves downwards in soil profiles from upslope recharge areas and eventually reappears at the surface in downslope discharge areas. As the excess water moves through the soil, it dissolves mineral salts. When an impermeable layer is encountered, the downward flow of water is restricted and obligated to flow laterally along the restricting layer into lower-lying slope positions. On lower-lying slope positions, the water discharges on the surface, where it evaporates and leaves the salts behind as a white crust.

Electromagnetic induction (EMI) has been used to detect groundwater recharge and discharge areas, and chart the distribution of soluble salts across landscapes. The apparent conductivity measured with an EMI sensor is principally affected by the soluble salt, clay, and water contents of soils (McNeill, 1980). However, in areas of saline soils, variations in soluble salt content is the principal factor affecting EC_a (William et al., 2006). Williams (1983) estimated that in saline soils, 70 % of the variation in EC_a can be explained by differences in the concentration of soluble salts alone.

Because of upward leaching and evaporative processes, salts are concentrated near the soil surface in groundwater discharge sites (seeps) (Richardson and Williams, 1994). The higher concentration of soluble salts in surface layers results in high EC_a and inverted salt profiles (EC_a is highest in surface layers and decreases with increasing depth). In general, discharge areas have higher EC_a than recharge areas.

Conversely, groundwater recharge sites are characterized by the downward leaching and concentration of salts at greater soil depths. As a consequence, EC_a is low in surface layers and increases with increasing depth (regular salt profile). In recharge areas, the low soluble salt and water contents are associated with low EC_a (Mankin and Karthikeyan, 2002).

Study Area:

The study area is located in the SW $\frac{1}{4}$, Section 4, Township 23 N, and Range 1 E. The study area is located in a cultivated field about 10.3 km southeast of Dutton in Teton County, Montana. Figure 2 is a soil map of the survey area from the Web Soil Survey⁵. Soil map units delineated within this quarter section include: Megonot silty clay loam, 0 to 4% slopes (70B); Pylon silty clay loam, 0 to 4% slopes (80B); Tanna clay loam, 0 to 4% slopes (82B); and Megonot-Tanna clay loams, 2 to 8% slopes (270).



Figure 2. This soil map is of the saline seep study area in Teton County, Montana.

The moderately deep, well drained Megonot, Pylon, and Tanna soils formed in residuum or alluvium weathered from semi-consolidated shale, siltstone or mudstone. These fine-textured soils are on

⁵ Soil Survey Staff, Natural Resources Conservation Service, United States Department of Agriculture. Web Soil Survey. Available online at <http://websoilsurvey.nrcs.usda.gov/>. Accessed [08/04/2013].

sedimentary uplands, hills and ridges. Tanna and Pylon soils have argillic horizons. Tanna soils have a mollic epipedon. The taxonomic classifications of these soils are listed in Table 1.

Table 1. Taxonomic classification of the named soils at the saline seep site in Teton County.

Soil Series	Taxonomic Classification
Megonot	Fine, smectitic, frigid Torrertic Haplustepts
Pylon	Fine, smectitic, frigid, Torrertic Haplustalfs
Tanna	Fine, smectitic, frigid Aridic Argiustolls

No mention of saline seeps is made for these soils and map units. Permeability of these soils is low and the underlying semi-consolidated, soft, sedimentary rock is assumed to form an aquitard, which restricts the downward flow of water and causes it to flow laterally towards lower-lying areas. Saline seeps develop on this landscape wherever the saline groundwater comes within about 1.5 m of the surface (Daniels, 1987). Saline seeps are characterized by prolonged periods of surface wetness, accumulation of salt crystals on the soil surface, and bare spots. Farm equipment can get stuck or cuts deep ruts through the sub-irrigated, wet seeps. Saline or wet spot symbols, if used to mark these areas on the original soil maps have been removed from modern digitized soil survey maps and only scant discussion of saline seeps are included in soil series or map unit descriptions. The unique and variable hydrology and morphology of soils in saline seeps is unrecorded.

Survey Protocol:

The USDA-ARS, U.S. Salinity Laboratory in Riverside, California, developed protocol for conducting field-scale soil salinity assessment with EMI (Corwin and Lesch, 2003, 2005a and 2005b). This protocol relies on the use of continuously recording EMI and GPS sensors mounted on mobile platforms to record spatial EC_a data. The ESAP (EC_e Sampling, Assessment, and Prediction) software was also developed by the USDA-ARS Salinity Laboratory to select optimal soil sampling locations and to predict soil salinity (EC_e) based on measured EC_a data (Lesch, 2005; Lesch et al., 2000, 1995a, 1995b). The methodology combines high-intensity EC_a data collection with sparse, low-density soil sampling. A goal of this prediction-based sampling approach is to reduce the number and optimize the collection of sampling data. Unfortunately, the ESAP programs are not compatible and completely operational on Windows 7. In the foreseeable future, it is very unlikely that any upgrade will be made to ESAP (Dennis Corwin personal communication on 24 June 2013).

Corwin and Lesch (2005b) stressed the need for standardized field procedures and guidelines for processing, interpreting, and displaying EC_a data, and to assure the reliability, consistency and compatibility of data. The following is a summary of the protocol that they have recommended for conducting field-scale EC_a surveys:

1. Obtain knowledge of site (e.g., soil map, conservation plans, and aerial photographs).
2. Collect georeferenced EC_a data.
3. Process EC_a data and prepare spatial images of data.
4. Based on spatial EC_a data, develop a sampling scheme. Select a set of georeferenced sample sites (6, 12, or 20 points) that are widely distributed across the entirety of the survey area and are also representative of the total variation of EC_a.
5. Collect small grab samples at the specified sample sites for the 0 to 30, 30 to 60, and 60 to 90 cm depth intervals (3 samples at each sample site).
6. Obtain laboratory analysis of saturated paste conductivity (EC_e) (and/or SAR; if needed) of each sample.
7. Statistical analysis of the EC_e (and/or SAR) and EC_a data. Determine correlations between EC_e and EC_a (or between SAR and EC_a) for each measured depth interval. Assess confidence levels.

8. Develop equations to predict EC_e (and/or SAR) from EC_a data for the different depth intervals. Use these equations to convert all EC_a data collected across the survey area into EC_e (and/or SAR).
9. Develop a GIS database for the graphic display of salinity and/or sodicity data.

When considering an EC_a survey of salinity, results will be improved if the survey can be conducted at a time of the year when the soil moisture condition is near field capacity (FC). As a general rule, surveys should be conducted when fields are at $\geq 70\%$ FC. Results will be substantially impacted when surveys are conducted at $< 50\%$ FC (Corwin and Lesch, 2005b).

In addition, EC_a will increase 1.9 % per 1 ° C increase in soil temperature. The soil temperature should be measured and the EC_a corrected to a standard temperature of 25 ° C. The EC_a measured at a particular temperature, t (in ° C) ($EC_{a,t}$), can be adjusted to a reference EC at 25 ° C ($EC_{a,25}$), using the following equations from Handbook 60 (U.S. Salinity Laboratory Staff, 1954; Table 15, p 90):

$$EC_{a,25} = ft \cdot EC_{a,t} \quad [1]$$

In equation [1], ft is a temperature conversion factor found in Table 15 of Handbook 60.

Results from the Teton County Site:

Not following the above-listed protocol, prior to completing an EMI survey of the study site, soil samples were obtained from 15 points surrounding a saline seep. However, due to excess wetness, the saline seep was not sampled. At each of the sampling points, small grab samples were collected from the 0 to 30, 30 to 60, and 60 to 90 cm depth intervals. These samples were sent to a commercial laboratory where their saturated paste conductivity (EC_e) was determined. At each of these sampling points, EC_a was measured with an EM38 meter in both the horizontal (HDO) and vertical (VDO) dipole orientations. The locations of the sampling points were obtained with a Garmin Map76 GPS receiver.

Table 2. Apparent conductivity (EC_a) and saturated paste conductivity (EC_e) data for the fifteen sample points at the Teton County study site.

ID	Longitude	Latitude	Altitude	EM38 VDO	EM38 HDO	ECe 0-30	ECe 30-60	ECe 60-90
028	-111.6182	47.7726	1152.26	158.0	120.0	4.0	8.2	10.9
030	-111.6178	47.7727	1154.90	125.0	101.0	3.9	7.2	8.8
031	-111.6169	47.7723	1154.66	128.0	95.0	3.2	6.0	8.6
032	-111.6174	47.7736	1152.50	122.0	97.0	3.7	6.7	8.5
033	-111.6160	47.7743	1156.58	108.0	89.0	3.7	6.3	7.6
034	-111.6164	47.7745	1155.38	131.0	104.0	3.9	7.3	9.2
035	-111.6166	47.7753	1156.58	133.0	99.0	3.3	6.3	8.9
036	-111.6174	47.7748	1154.66	117.0	89.0	3.2	5.7	7.9
037	-111.6185	47.7756	1162.11	130.0	110.0	4.7	8.5	9.5
039	-111.6181	47.7744	1159.71	152.0	115.0	3.9	7.7	10.4
040	-111.6196	47.7747	1160.19	103.0	91.0	4.3	7.1	7.6
041	-111.6202	47.7748	1158.99	113.0	95.0	4.1	7.0	8.1
042	-111.6183	47.7736	1157.30	171.0	126.0	3.9	8.4	11.6
043	-111.6193	47.7735	1159.23	167.0	133.0	4.9	9.9	11.9
044	-111.6186	47.7730	1162.11	149.0	101.0	2.9	5.8	9.5

Table 2 lists the GPS and EMI measurements recorded at the fifteen soil sampling points and the data from the soil salinity analysis. In Table 2, each sample is identified by an identification number (ID).

Apparent conductivity (mS/m) measured with an EM38 meter in the VDO and HDO are listed in columns 5 and 6, respectively. Columns 7, 8, and 9, list the salinity (dS/m) for the 0 to 30, 30 to 60, and 60 to 90 cm depth intervals, respectively.

As evident in Table 2, both EC_a and EC_e increased and became more variable with increasing soil depths. All salt profiles measured with the EM38 meter were regular (EC_a increasing with increasing soil depth). At no sampling point was an inverted salt profile encountered; inverted salt profiles are often indicative of saline seeps. Apparent conductivity measured in the shallower-sensing HDO averaged 104 mS/m and ranged from 89 to 133 mS/m. Apparent conductivity measured in the deeper-sensing VDO averaged 134 mS/m and ranged from 103 to 171 mS/m. For the 0 to 30 cm depth interval, EC_e averaged 3.8 dS/m and ranged from 2.9 to 4.9 dS/m. Ten of the fifteen samples had non-saline (> 4 dS/m) surface layers. For the 30 to 60 cm depth interval, EC_e averaged 7.2 dS/m and ranged from 5.7 to 9.9 dS/m. Ten of the fifteen samples from this depth interval were moderately saline (4 to < 8 dS/m); five of the samples were non-saline. For the 60 to 90 cm depth interval, EC_e averaged 9.3 dS/m and ranged from 7.6 to 11.9 dS/m. Twelve of the fifteen samples from this depth interval were moderately saline; three of the samples were non-saline. In general, these measured EC_e values were considered low and not entirely representative of a saline seep.

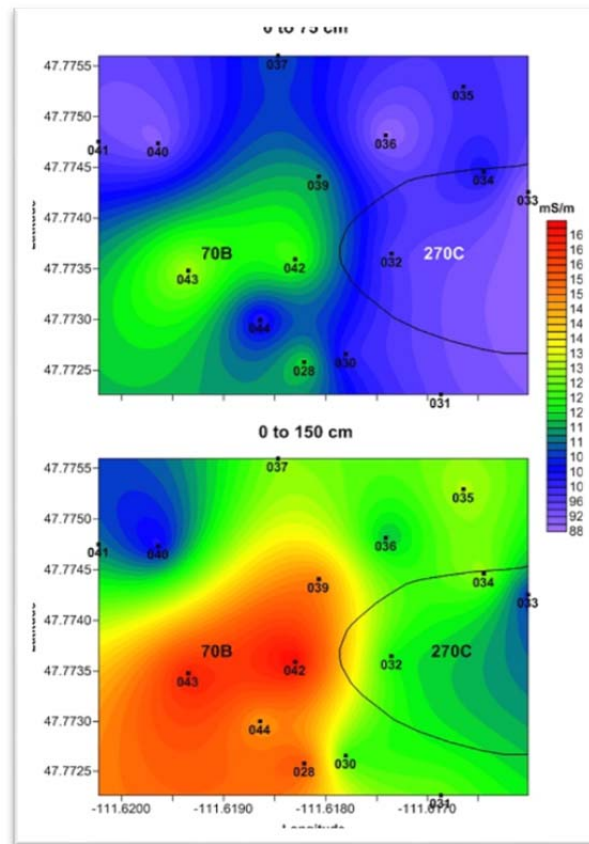


Figure 3. These plots of EC_a data are from the area that was sampled at the Teton County Site. Apparent conductivity data were collected with an EM38 meter operated in the horizontal (upper plot) and vertical (lower plot) dipole orientations.

Figure 3, contains plots of EC_a data collected within the sampled area. For comparative purposes, the same color scale and scheme are used in each plot. In Figure 3, the upper and lower plots represent

spatial EC_a data measured in the shallower-sensing HDO and the deeper-sensing VDO, respectively. In each plot, spatial patterns have been interpolated from the data measured at the 15 sample sites. The location and identity of each sample point is shown in Figure 3. The soil line has been imported from the Web Soil Survey.

In Figure 3, spatial patterns indicate an area of higher EC_a located in the southwest corner of the sample area. Though very weakly expressed and spatially confined in the data collected in the shallower-sensing HDO, the area of higher EC_a expands in size and amplitude with the increasing depth profiled in the VDO.

Correlations were derived for the measured EC_a and EC_e data shown in Table 2. Because of the small sample size (15 samples), non-parametric Spearman's rank correlation coefficients were determined (see Table 3). Strong and significant correlations were obtained between EC_a and the EC_e of the 30 to 60, 60 to 90, and 0 to 90 cm depth intervals. For EC_a measured in the VDO, a strong and significant correlation was only obtained with the EC_e of the 60 to 90 cm depth interval. The lack of stronger correlations is ascribed to the lower than ideal field capacity of the soils, and variations in moisture and clay contents across the sample area.

Table 3. Spearman's rank correlation coefficients for the sampled EC_a and EC_e data.

	EC_e 0-30	EC_e 30-60	EC_e 60-90	EC_e 0-90
HDO	0.4634	0.8152*	0.9705*	0.8991*
VDO	0.1107	0.5330	0.9696*	0.6606

* Significant at the .0001 level.

Based on the results of the statistical analysis, the following predicative equations were developed to convert EC_a data into measurements of EC_e :

$$EC_e \text{ 0 to 30 cm} = 3.31 + (0.004 \times EC_a) \quad [2]$$

$$EC_e \text{ 30 to 60 cm} = 2.69 + (0.034 \times EC_a) \quad [3]$$

$$EC_e \text{ 60 to 90 cm} = 0.77 + (0.064 \times EC_a) \quad [4]$$

$$EC_e \text{ 0 to 30 cm} = 2.22 + (0.034 \times EC_a) \quad [5]$$

In each of these equations, EC_a is the apparent conductivity measured with the 100-cm intercoil spacing of the EM38-MK2 meter operated in the VDO. When operated in the VDO, the 100-cm intercoil spacing provides a similar depth-weighted response as the EM38 meter (operated in the VDO). Measurements recorded with the 50-cm intercoil spacing were corrupted and could not be used. Although the derived correlations (Table 3) were higher and more significant for measurements obtained in the HDO, the correlations obtained in the VDO were considered acceptable.

A detailed EMI survey of the 160 acre field was completed using a mobile platform with an EM38-MK2 meter (operated in the VDO) towed in a plastic sled. The field was traversed from side to side in a north-south direction at speeds of about 3 to 5 m/hr. Twenty-six traverse lines, each spaced about 30 m apart, were completed across the field. Data were recorded at a rate of two measurements per second. Based on 11426 EC_a measurements, for the nominal depth of investigation of 0 to 150 cm, EC_a averaged 101.9 mS/m and ranged from about 42 to 344 mS/m across the study site. However, one-half of the measurements were between about 74 and 119 mS/m.

Figure 4, contains a plot of the EC_a data collected at the Teton County site. This plot is based on 11,426 EC_a measurements. In this plot, the locations of the 15 sampling points used to construct the EC_a images in Figure 3 are shown. Segmented lines outline the area that is shown on the EC_a plots in Figure 3. In

Figure 4, several seeps, with $EC_a > 150$ mS/m, appear to be arranged in a discontinuous, sinuous pattern that meanders across the survey area from the southwest to the northeast corner. These seeps appear to follow the 1158 m contour line and are border to the north or west by more steeply sloping gradients. Also evident in this plot are lines of relatively high EC_a that extend in a west-northwesterly and upslope direction away from these seeps. These are believed to represent flow paths. The area encompassed by these flow lines appears to be more extensive than the seep areas themselves. These lines may represent preferential channels for excess water to drain from recharge areas (located on higher-lying areas to the west and north).

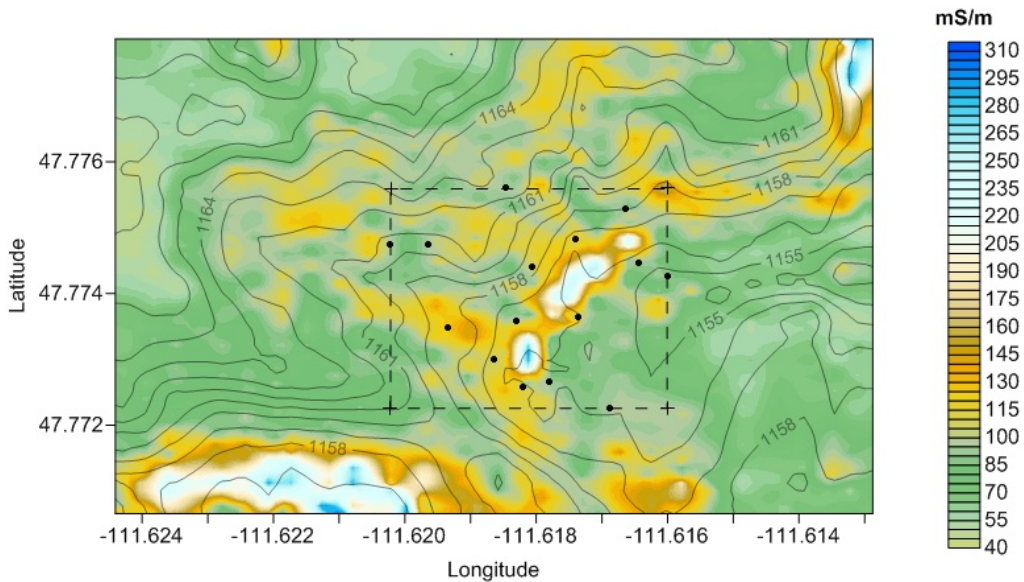


Figure 4. This plot shows the spatial distribution of EC_a for the upper 0 to 150 cm of the soil across the Teton County site. Contour lines are expressed in m above msl. Soil sampling points (•) and sampling area (Figure 3) are shown.

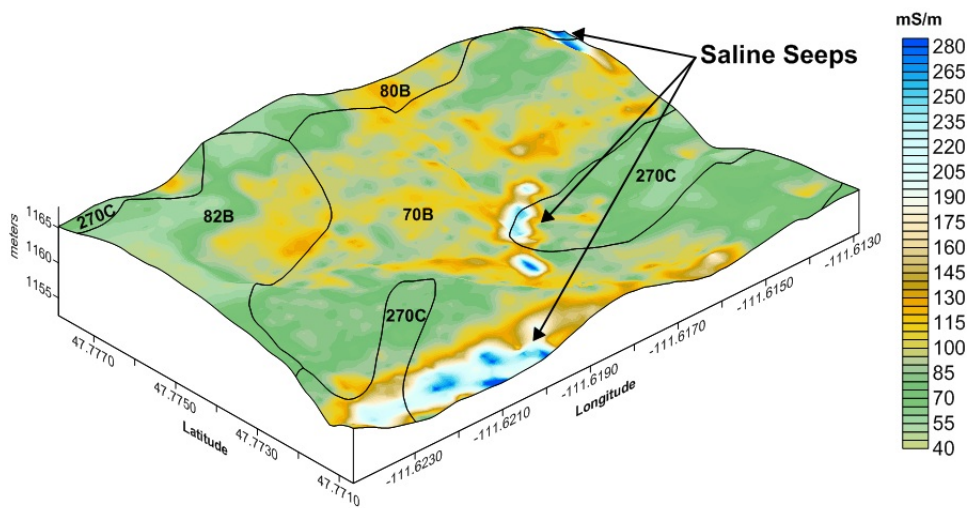


Figure 5. This 3D simulation shows the spatial distribution of EC_a for the upper 0 to 150 cm of the soil across the Teton County site. Elevation data used in this simulation were obtained by GPS

The spatial relationship of recharge, discharge and flow-through areas are further illuminated in the three-dimensional (3D) image shown in Figure 5. The elevation data used to construct the underlying wireframe image were collected with the Trimble AgGPS 114 L-band DGPS antenna. The overlying contour plot of EC_a data is the same as shown in Figure 4. Major saline seeps have been identified in Figure 5. Figure 5 provides a more vivid picture of the complex relationship among relief, recharge areas and seeps. The extent and recharge directions for the seeps may be evident in this simulation. For example, for the seep in the central part of the survey area, flow lines appear to be more extensive and numerous in the area to the west and north and less in the area to the east and southeast.

Using predicative equations [2], [3], and [4], the 11,426 EC_a measurements were converted into measures of soil salinity (dS/m). Figure 6 contain plots of the predicted EC_e . These plots are based on data generated from equations that were developed from the sampled soil EC_e and EC_a data. These equations were used to convert the raw EC_a data collected at this site into EC_e . For comparative purposes, the same color scale and intervals have been used in all of these plots of EC_e data.

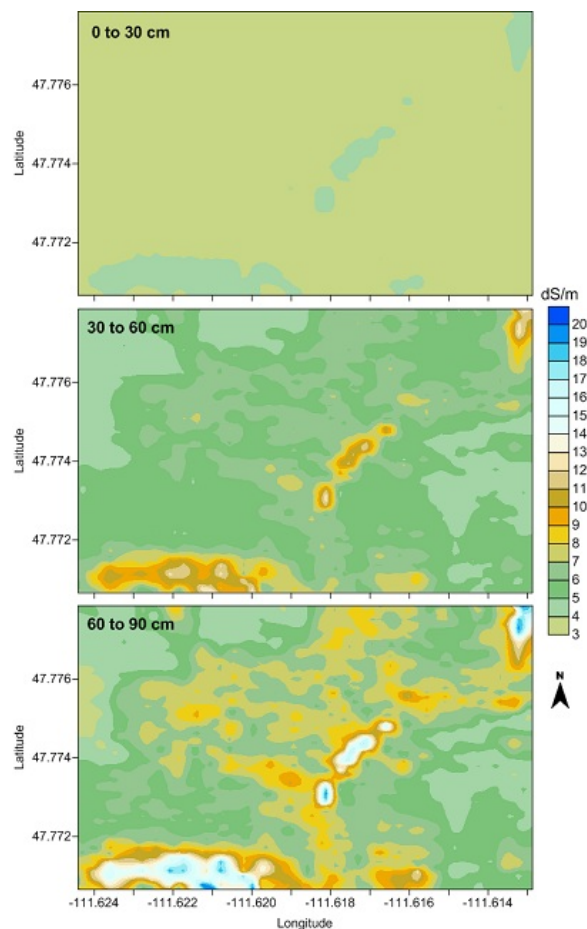


Figure 6. These plots of salinity were prepared using predictive equations for the 0 to 30 (upper plot), 30 to 60 (middle plot) and 60 to 90 (lower plot) cm depth intervals and the EC_a measurements collected at the Teton County site.

As evident in the modeled data shown in Figure 6, salinity increases with increasing soil depth. However, the distribution of soluble salts and the level of soil salinity is both depth and spatially variable.

Apparent conductivity maps are valuable tools to management as they show the locations of not only established, but emergent saline seeps and the connectivity among them. Areas with low EC_a represent

areas of vertical recharge. Here, infiltrating water leach soluble salts deeper in soil profiles. On the other hand, areas with high EC_a are associated with high discharge rates and salt accumulation.

References:

Corwin, D.L., and Lesch, S.M., 2003, Application of soil electrical conductivity to precision agriculture: Theory, principles, and guidelines: *Agron. J.*, 95, 455–471.

Corwin, D.L., and Lesch, S.M., 2005a. Apparent soil electrical conductivity measurements in agriculture: *Comput. Electron. Agric.*, 46(1–3) 11–43.

Corwin, D.L., and Lesch, S.M., 2005b, Characterizing soil spatial variability with apparent soil electrical conductivity: I. Survey protocols: *Comput. Electron. Agric.*, 46(1–3) 103–133.

Daniels, R.B., 1987. Saline seeps in the Northern Great Plains of the USA and the southern prairies of Canada. 381-406 pp. In: Wolman, M.G., and F.G.A. Fournier (eds.) *Land Transformation in Agriculture*. John Wiley and Sons, Ltd.

Lesch, S.M. 2005. Sensor-directed response surface sampling designs for characterizing spatial variation in soil properties. *Computers and Electronic in Agriculture* 46: 153-180.

Lesch, S.M., J.D. Rhoades and D.L. Corwin. 2000. ESAP-95 version 2.10R User Manual and Tutorial Guide. Research Report 146. USDA-ARS George E. Brown, Jr. Salinity Laboratory, Riverside, California.

Lesch, S.M., D.J. Strauss and J.D. Rhoades. 1995a. Spatial prediction of soil salinity using electromagnetic induction techniques. 1. Statistical prediction models: A comparison of multiple linear regression and cokriging. *Water Resources Research*. 31:373-386.

Lesch, S.M., D.J. Strauss and J.D. Rhoades. 1995b. Spatial prediction of soil salinity using electromagnetic induction techniques. 2. An efficient spatial sampling algorithm suitable for multiple linear regression model identification and estimation. *Water Resources Research* 31:387-398.

Mankin, K.R., and R. Karthikeyan, 2002. Field assessment of saline seep remediation using electromagnetic induction. *Transaction of ASAE* 45(1): 99-107.

McNeill, J.D., 1980. Electromagnetic terrain conductivity measurements at low induction numbers. Technical Note TN-6. Geonics Ltd., Mississauga, Ontario.

Richardson, D.P. and B.G. Williams, 1994. Assessing discharge characteristics of upland landscapes using electromagnetic induction techniques. Technical memorandum 94/3. CSIRO Institute of Natural Resources and Environment, Division of Water Resources. Canberra, Australia. 10 p.

U.S. Salinity Laboratory Staff, 1954. Diagnosis and improvement of saline and alkali soils, USDA Handbook 60. U.S. Government Printing Office, Washington, DC, USA, pp. 1–160.

Williams, B.G., 1983. Electromagnetic induction as an aid to salinity investigations in North East Thailand. Technical Memorandum 83/27. CSIRO Institute of Biological Resources, Division of Water and Land Resources. Canberra, Australia.

Williams, B.G., J. Walker, and J. Anderson, 2006. Spatial variability of regolith leaching and salinity in relation to whole farming planning. *Australian Journal of Experimental Agriculture* 46: 1271-1277.